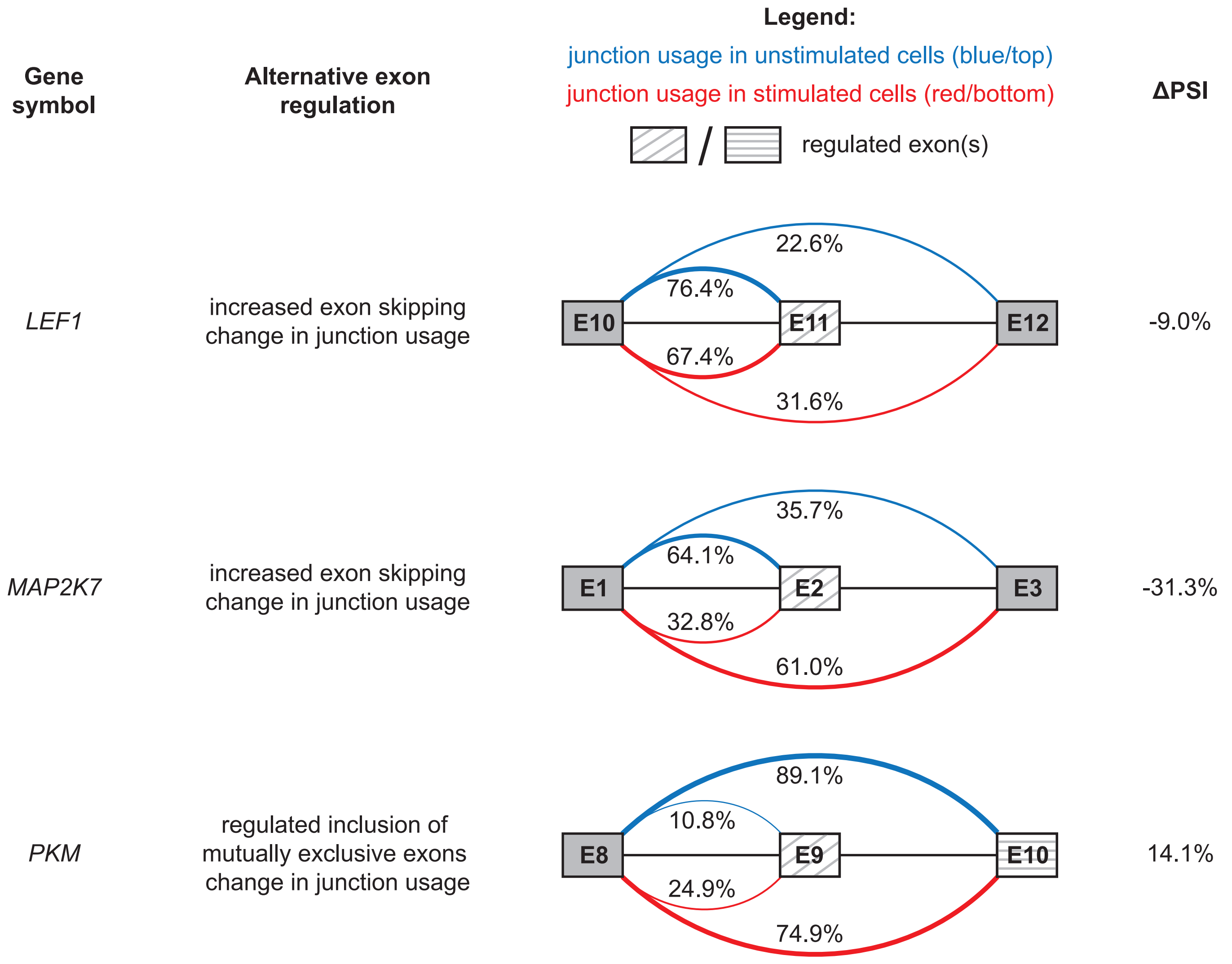

Supplemental Figure S1. Visualization of local splice variations (LSVs). Examples given for three genes with the status of exon usage and effect on alternative exon inclusion for each gene upon T cell stimulation. Schematics representing the alternative junction (AJ) usage patterns for the genes are shown to the right. Junction usage is represented by the thickness of the dashed lines (most highly used exon junction has a thicker line) and splicing pattern in unstimulated and stimulated T cells is shown is shown in blue and red, respectively.

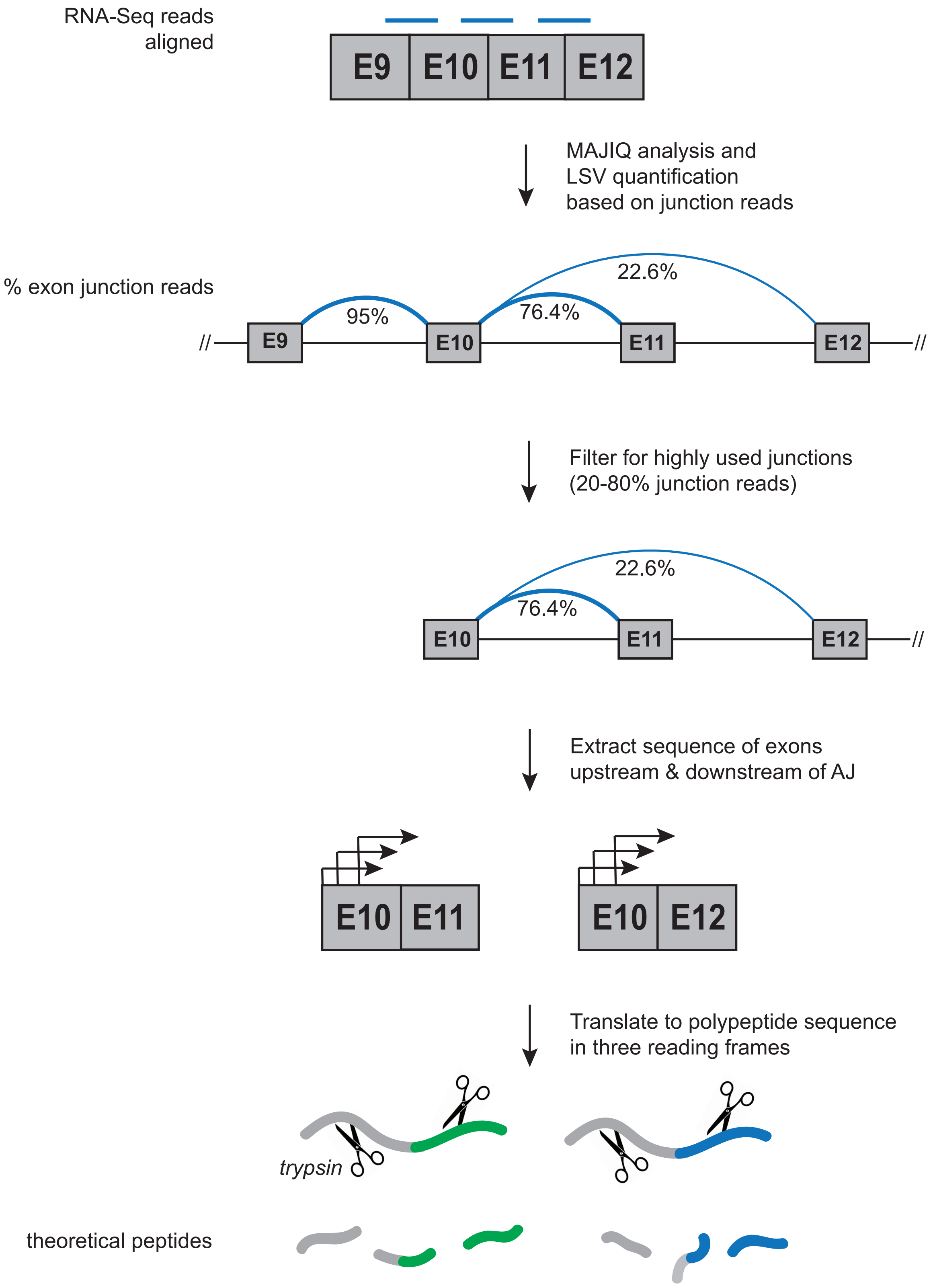

Supplemental Figure S2. Schematic workflow for generating custom database based on RNA-seq data. RNA-seq data was analyzed with MAJIQ to identify local splice variations (LSVs) and quantify changes in exonic splicing patterns. MAJIQ output was filtered for LSVs that had two or more junctions, each with 20-80% of reads going to/coming from a specific junction ('alternative junction', AJ). The flanking exonic sequences upstream and downstream of a given AJ were then extracted and the exon triplet was translated in silico using three forward reading frames.

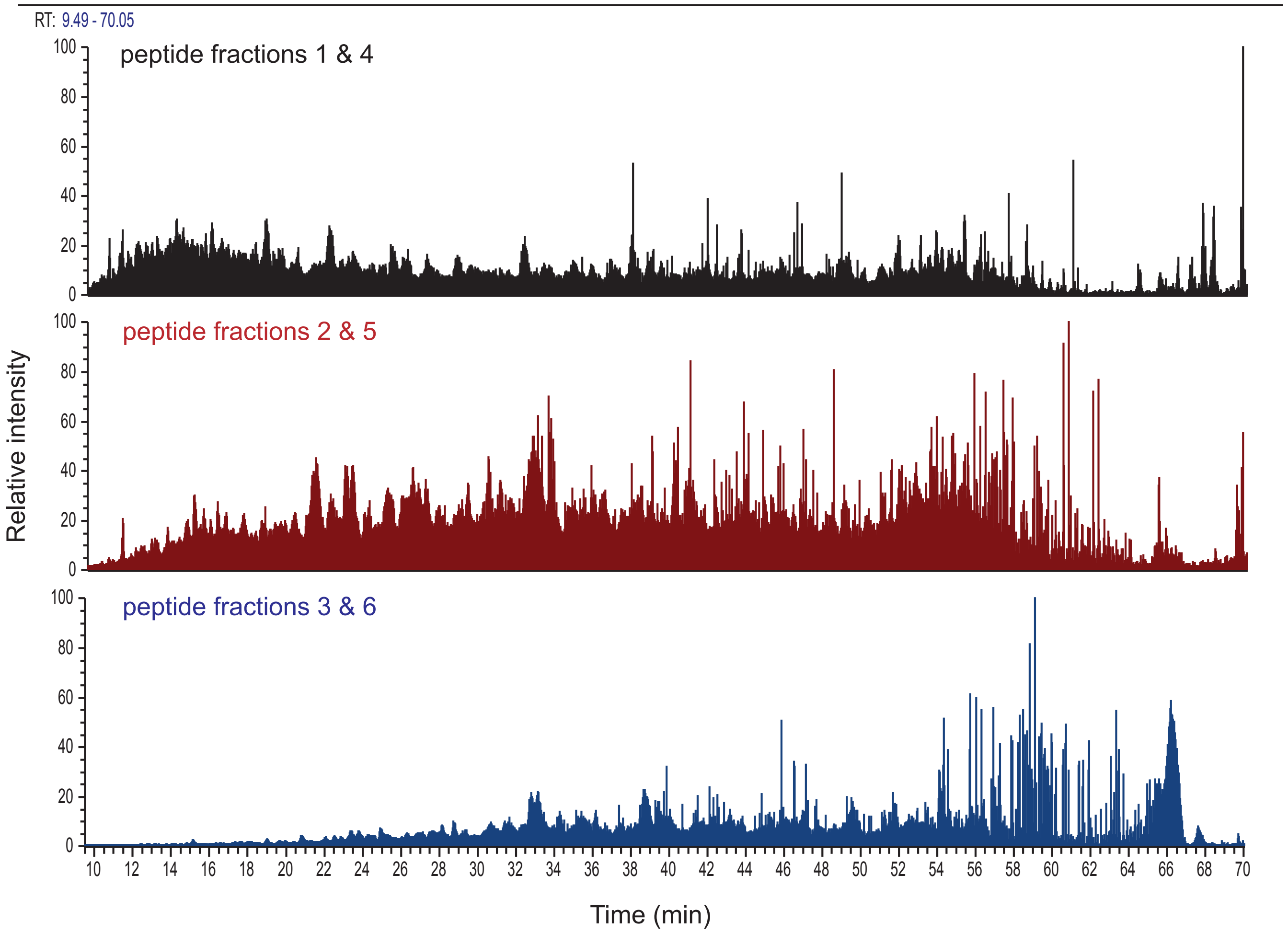

Supplemental Figure S3. Validation of peptide high-pH fractionation. Overlaid total ion chromatogram (TIC) traces from DIA Acquisition of pooled high-pH peptide fractions from a representative sample.

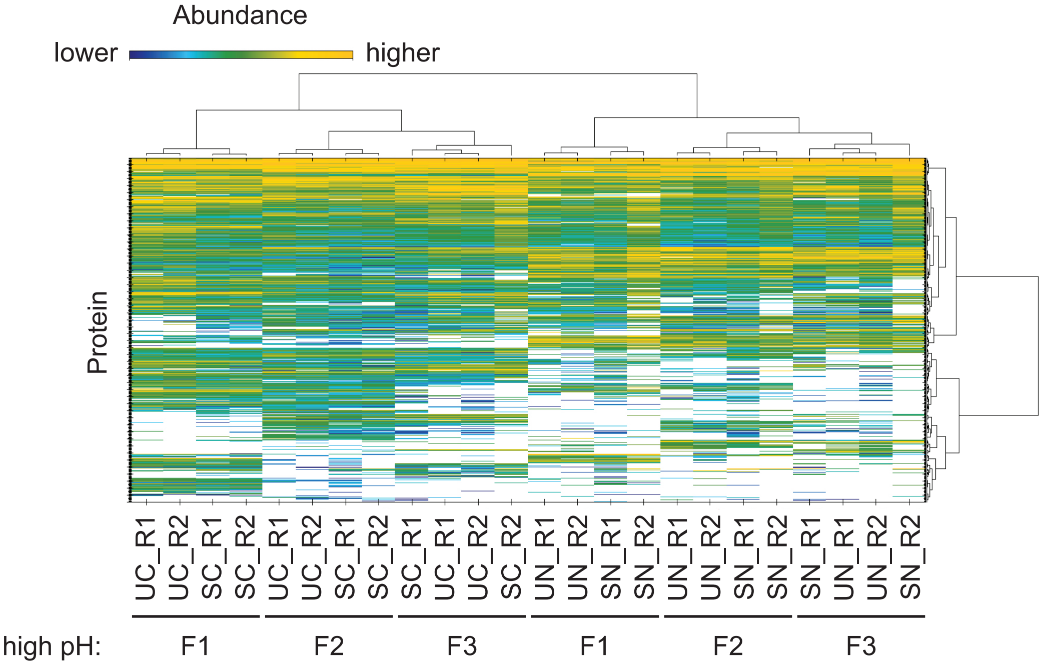

Supplemental Figure S4. Heatmap of high-pH peptide fractionation samples showing high reproducibility by co-clustering of samples based on high-pH and sub-cellular fractions. Classifications: T cell stimulation state (U= unstimulated, S= stimulated), sub-cellular fraction (C= cytoplasmic, N= nuclear), high-pH fraction (F1 = fraction 1, F2= fraction 2, F3= fraction 3, see also Supplemental Table S1), biological replicates (R1= replicate 1, R2= replicate 2). Abundance color key: low to high protein abundance is reflected by deep blue to yellow color gradient; white = not detected.

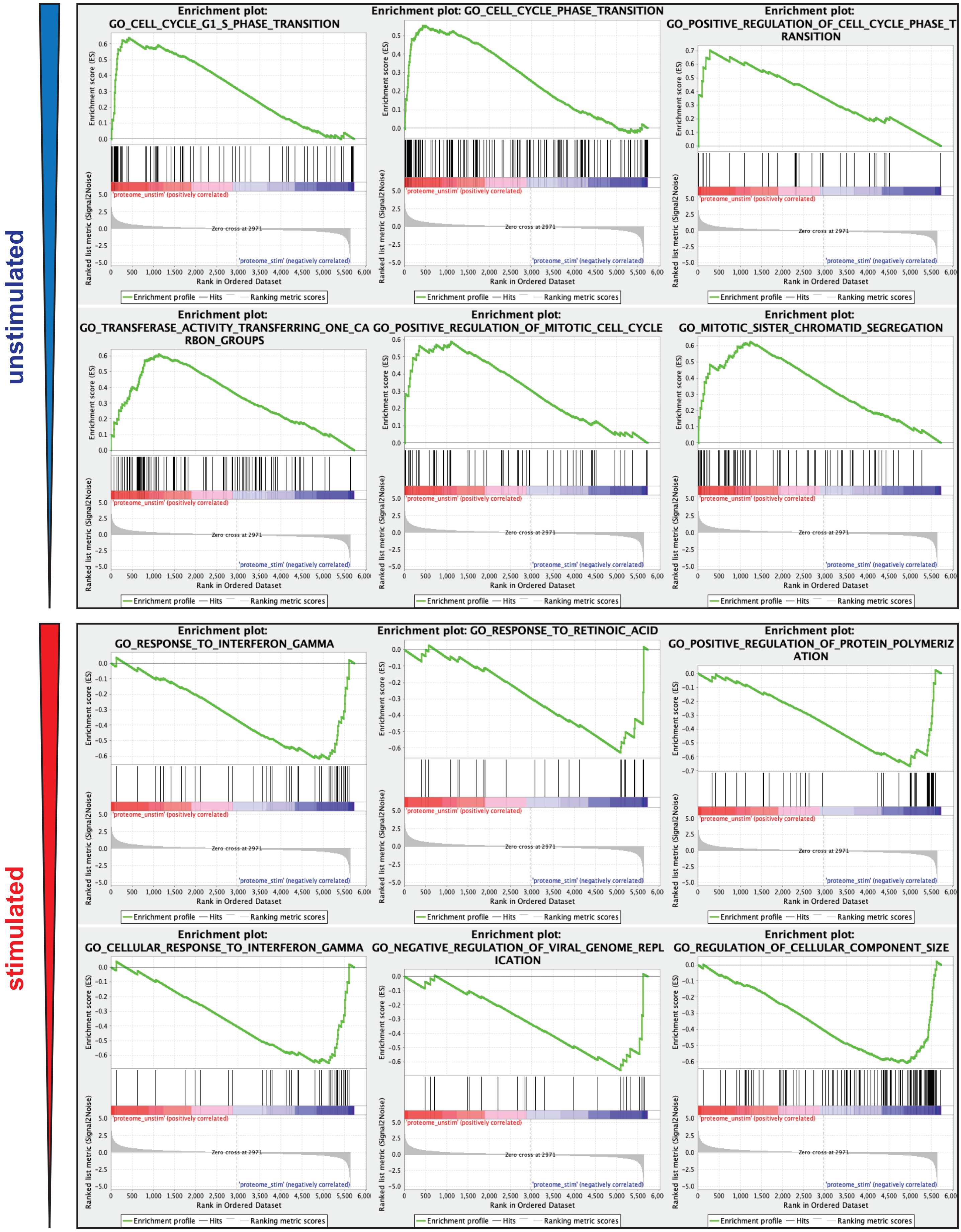

Supplemental Figure S5. Protein gene set enrichment analysis (GSEA) enrichment plots for the top 6 Gene Ontology (GO) categories in unstimulated and stimulated T cell conditions.

PKM1 EJP (from E9 inclusion/E10 skipping)

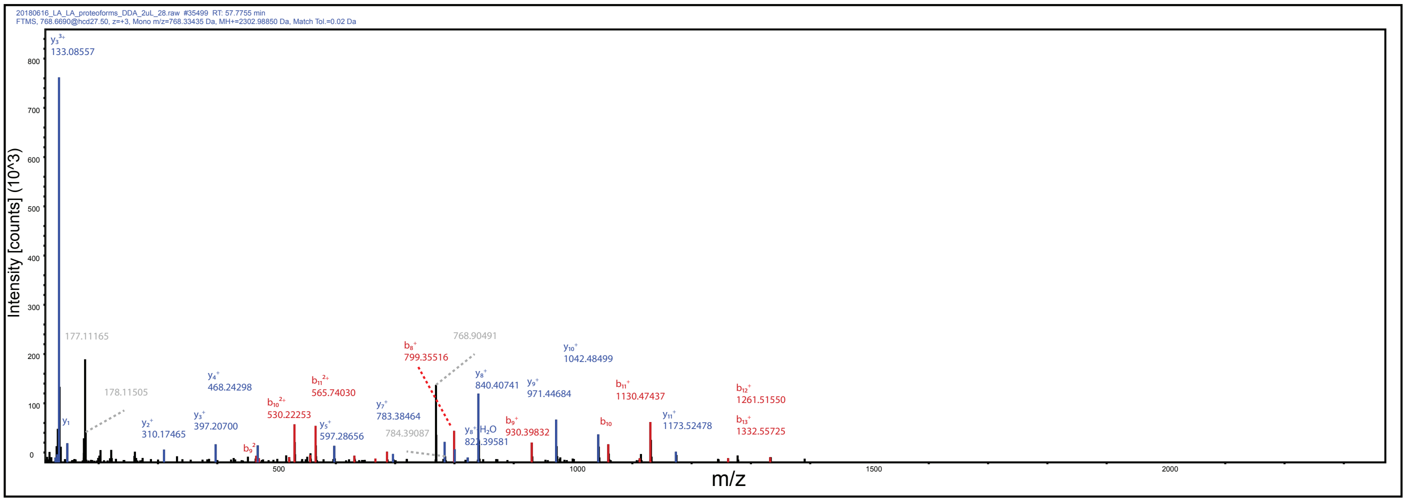

PKM2 EJP (from E9 skipping/E10 inclusion)

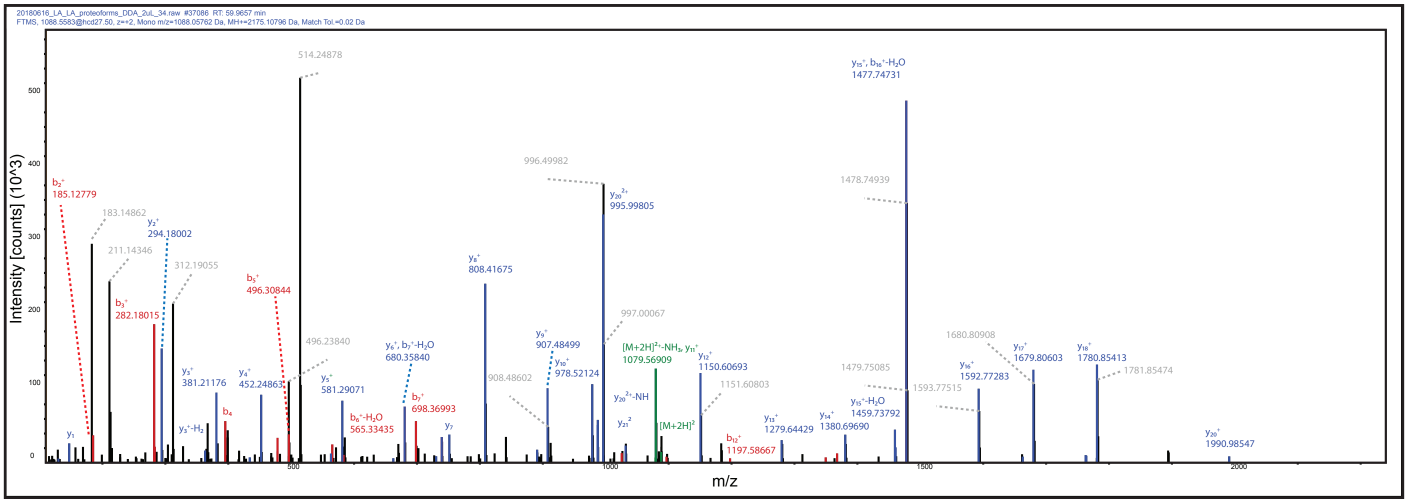

Supplemental Figure S6. MS^2 fragmentation spectra for PKM1/2 exon junction peptides (EJPs). Data was acquired using a nano-liquid chromatography coupled online with a Q Exactive HF-X mass spectrometer instrument set to data-dependent acquisition (DDA) and positive polarity mode. Fragment *b*- and *y*-ions were generated by high-collision induced dissociation (HCD) and detected on the orbitrap with 30,000 resolution. Xcalibur software was used for data collection.

LEF1-E11 EJP (from E11 inclusion)

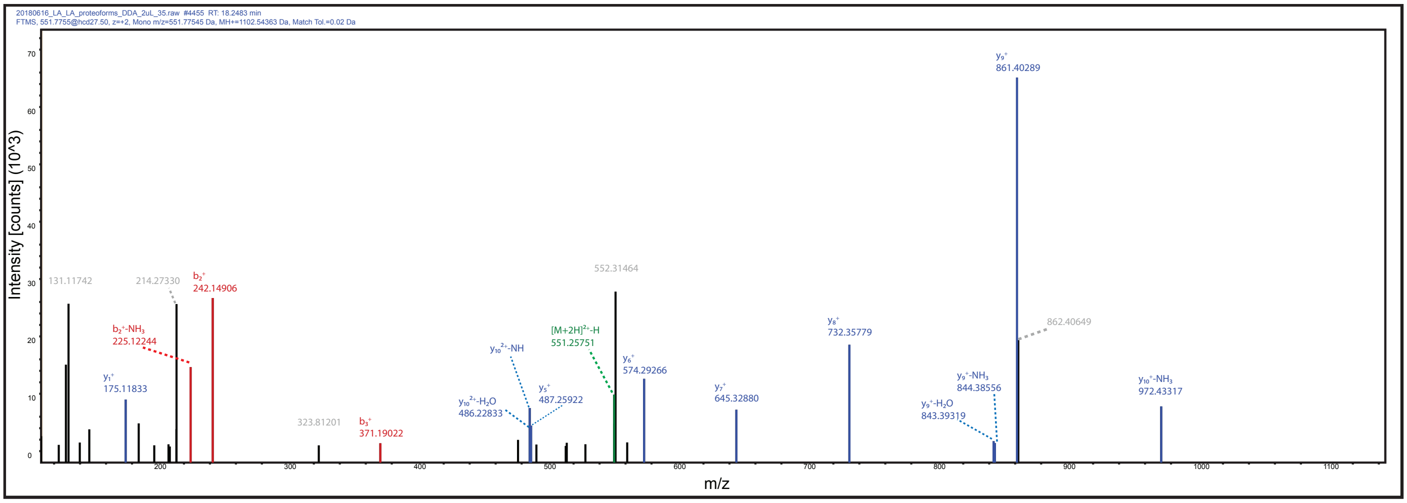

LEF1-E12 EJP (from E11 skipping)

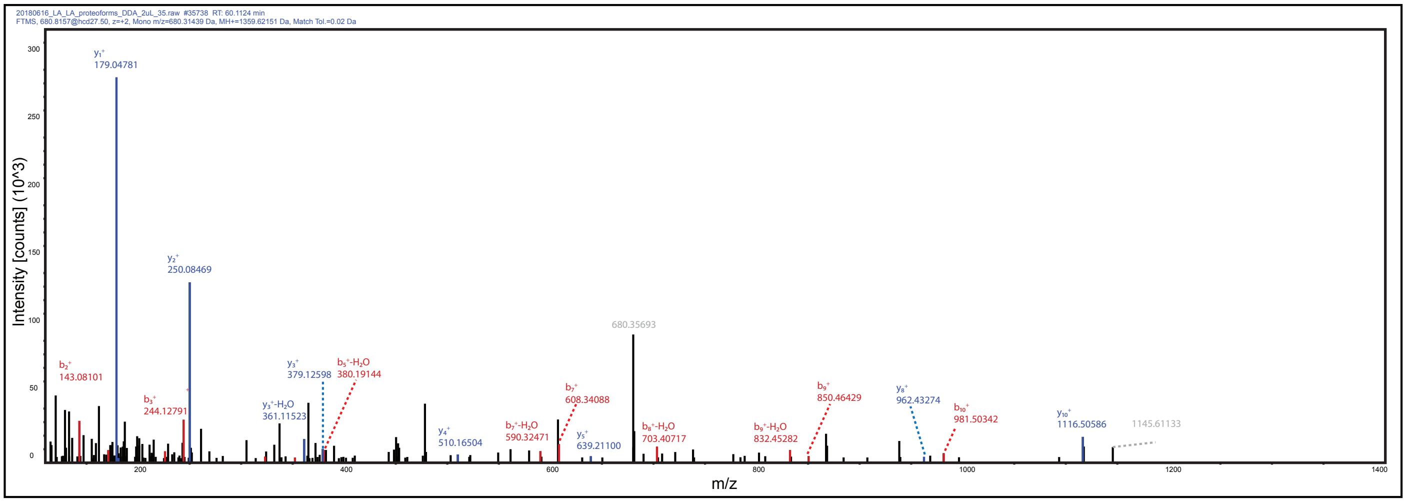

Supplemental Figure S7. MS^2 fragmentation spectra for LEF1 exon junction peptides (EJPs). Data was acquired using a nano-liquid chromatography coupled online with a Q Exactive HF-X mass spectrometer instrument set to data-dependent acquisition (DDA) and positive polarity mode. Fragment *b*- and *y*-ions were generated by high-collision induced dissociation (HCD) and detected on the orbitrap with 30,000 resolution. Xcalibur software was used for data collection.